Skillful seasonal prediction of key carbon cycle components: NPP and fire risk

Philip E Bett[1], Karina E Williams[1,2], Chantelle Burton[1], Adam A Scaife[1,3], Andrew J Wiltshire[1] and Richard Gilham[1]

[1] Met Office Hadley Centre, FitzRoy Road, Exeter EX1 3PB, UK
[2] Global Systems Institute, University of Exeter, Laver Building, North Park Road, Exeter EX4 4QE, UK
[3] College of Engineering, Mathematics and Physical Sciences, Exeter University, Exeter, UK

E-mail: philip.bett@metoffice.gov.uk

14 September 2019, r8543

Abstract. Seasonal forecasts of global CO_2 concentrations rely on the well-documented relationship with the El Niño–Southern Oscillation (ENSO), combined with estimated anthropogenic emissions. Here, we investigate the skill of the GloSea5 seasonal forecasting system for two carbon cycle processes that underlie the global CO_2–ENSO relationship: the impact of meteorological conditions on CO_2 uptake by vegetation (characterised by net primary productivity, NPP), and on fire occurrences (characterised by fire risk indices). In the tropics, during El Niño events, CO_2 uptake by vegetation is reduced and fires occur more frequently, leading to higher global CO_2 levels.

We use the McArthur forest fire index, calculated from daily data from several meteorological variables. We also assess a simpler fire index, based solely on seasonal mean temperature and relative humidity, since seasonal forecasts based on simpler combinations of model output (fewer input variables, averaged over longer periods/larger regions) can be more skillful than more complicated metrics, which retain more noise.

For NPP, the skill is high in regions that respond strongly to ENSO, such as equatorial South America in boreal winter, and northeast Brazil in boreal summer. There is also skill in some regions without a strong ENSO response. For the fire risk indices, there is significant skill across large parts of the tropics, including in Indonesia, southern and eastern Africa, and parts of the Amazon Basin. We relate this skill to the underlying meteorological variables, finding that fire risk in particular follows similar patterns to relative humidity.

On the seasonal-mean timescale, the McArthur index offers no benefits over the simpler fire index: they show the same relationship to burnt area and response to ENSO, and the same levels of skill, in almost all cases. Our results highlight potentially useful prediction skill, as well as important limitations, for seasonal forecasts of land-surface impacts of climate variability.

Keywords: Carbon cycle, seasonal forecasting, net primary productivity, fire risk
Submitted to: *Environ. Res. Commun.*

1. Introduction

Atmospheric CO_2 levels are often considered to be a 'driver' of changes in the climate system, particularly when considering projected changes over many decades. However CO_2 concentration is itself a function of both anthropogenic emissions and exchanges with the land and ocean. It is these natural fluxes in particular that drive the interannual variability. It has been shown that CO_2 concentrations can be skilfully predicted from features of the climate system, such as the El Niño–Southern Oscillation (ENSO) together with an estimate of anthropogenic emissions (Jones et al., 2001, Jones and Cox, 2005, Betts et al., 2016, 2018).

ENSO is the largest global mode of interannual variability and affects both the global climate and global carbon cycle (Rodenbeck et al., 2018). El Niño and La Niña events occur every 2–7 years, when sea surface temperatures (SSTs) in the equatorial Pacific are anomalously high or low, respectively, over a period of several months (e.g. Philander, 1990, Trenberth, 1997). The anomalies typically peak in boreal winter, but their impacts on the climate can last for many months. An El Niño event brings higher temperatures and reduced precipitation to the tropics. These conditions put vegetation and soils under stress, with implications for their large global stores of carbon: it leads to increased respiration, reduced assimilation of carbon, and increased fire risk (Kim et al., 2016, Chen et al., 2016). The three factors of heterotrophic respiration, vegetation productivity, and fire variation, dominate the interannual variability of CO_2 (Zeng et al., 2005).

Fire emissions in pan-tropical forests increased by over 100% during El Niño compared to La Niña from 1997 to 2016 (Chen et al., 2017), and a one-third increase in fires in the Brazilian Amazon was recorded during the 2015/16 El Niño (Aragao et al., 2018). The spike in fire emissions in 1997/98, associated with a large El Niño event, has been attributed to the burning of large areas of carbon-rich peatland in Indonesia (Page et al., 2002), contributing between 0.81 Gt and 2.57 Gt of carbon to global annual emissions, the equivalent of 13–40%.

Tropical forests are not typically at high risk of burning due to high moisture levels. However, during years of strong drought such as during an El Niño, vegetation can dry out enough to burn. On top of a background of continued warming, these events may have increasing impacts on fire risk in the future (Fasullo et al., 2018). An ignition source is also required to start a fire, either via anthropogenic or natural means (e.g. lightning), and with increased land use activities in recent decades, including the use of fire as a land-clearance method, the risk of fire has also been increasing (Spessa et al., 2015).

The variation in vegetation carbon uptake/emissions within a system can be assessed in terms of net primary production (NPP). This represents the amount of CO_2 that is taken in by vegetation, calculated as gross primary production (GPP, the total amount of carbon assimilated by plants) minus carbon lost through autotrophic respiration (Roxburgh et al., 2005). Kim et al. (2016) studied Earth System Models (ESMs) from CMIP5 and showed that the CO_2–ENSO relationship in the models is mostly due to variations in NPP: the increased temperature and reduced precipitation in the tropics due to an El Niño event leads to a reduction in NPP, which leads to an increase in atmospheric CO_2. They found that their ESM ensemble overestimated ENSO-related NPP anomalies, due to overestimating the temperature response to ENSO. However, the ESMs also tended to underestimate the carbon fluxes from fires, and from heterotrophic respiration, which adds to the uncertainty in the simulation

of the CO_2–ENSO relationship.

ENSO can be forecast with a high degree of skill using seasonal climate prediction systems (e.g. Barnston et al., 2012, Ren et al., 2019, and references therein). Various authors have studied how this can be used to forecast fires in different regions. For example, Chen et al. (2016) examined how SST indices, including ENSO, can be used to forecast annual burnt area across the globe. Chen et al. (2011) performed a similar study, focusing on South America. Spessa et al. (2015) demonstrated that fire activity is negatively correlated with rainfall, and positively associated with deforestation in Indonesia. They use rainfall from a seasonal forecasting system to show that burnt and fire-affected area in Indonesia can be forecast at several months lead time, and that these results are strongly influenced by El Niño events. Mariani et al. (2016) evaluated the correlation between ENSO and seasonal rainfall anomalies across Southeast Australia. They found a significant and persistent influence of El Niño on fire activity in the region on a decadal scale, mostly driven by an ENSO-related reduction in water availability. The increased activity is influenced not only by drier conditions in the austral summer and autumn of the fire season year, but also by water availability in the preceding winter and spring.

Betts et al. (2016, 2018) successfully forecast the CO_2 concentrations at Mauna Loa, often regarded as a proxy for global levels, based on the observed CO_2–ENSO relationship and estimated anthropogenic emissions. Their hybrid statistical–dynamical approach used a forecast of the Niño3.4 index of SSTs in the east Pacific, from the GloSea5 seasonal forecasting system.

GloSea5 is based on a coupled climate model, which includes simulation of the land surface and vegetation in its JULES (*Joint UK Land Environment Simulator*) component model (Best et al., 2011, Clark et al., 2011). Although GloSea5 does not include a coupled carbon cycle, JULES calculates NPP internally. Fire risk indices can also be calculated offline, based on GloSea5 forecast model output. We are therefore able to examine how well the same seasonal forecasting system can directly model separate elements of the carbon cycle.

Human-relevant impacts of weather and climate variability are often described using complex physical or statistical models, requiring driving data from several different quantities at sub-daily time resolution. These can be effective for short-term forecasting (e.g. weather timescales) and case studies of past events or historical climatology. However, for seasonal climate forecasting, this kind of comprehensive impact modelling is usually not effective: using a metric based on fewer variables, driven by data averaged over longer timescales, will tend to be less noisy and more skillful. Bett et al. (2019) demonstrate this explicitly in the context of wind and solar energy generation in Europe, following similar work by Palin et al. (2016) and Clark et al. (2017). A balance therefore has to be made between capturing the processes necessary to forecast the interannual variability of the quantity of interest, without simply adding complexity to a model where there is insufficient skill. In the context of the interannual variability of crop yield, Williams and Falloon (2015) demonstrated that the driving data to their crop model can be simplified: replacing some variables with climatologies, and reducing the temporal resolution of others, did not reduce the predictability. In the context of fire forecasting, Turco et al. (2018) looked at combinations of precipitation, evapotranspiration and temperature as predictors for seasonal forecasts of burnt area. They found that using a solely precipitation-based metric was the best choice.

In this paper we assess the skill of GloSea5 for forecasting NPP and the McArthur

Forest Fire Danger Index (McArthur, 1966, Luke and McArthur, 1978) in the Tropics, and explain this with reference to the skill in the underlying meteorological variables. We also investigate a simple fire index based only on temperature and relative humidity, to understand the impact of using fewer and simpler quantities in the calculation of fire risk on seasonal time scales.

We describe the data sets, methods and calculations we use in our analysis in section 2. Section 3 describes our results, firstly validating our observation-based data, then considering seasonal forecast skill. We discuss our conclusions in section 4.

2. Data and analysis methods

2.1. Fire risk indices

Fire indices are used operationally in many fire-prone regions to help risk reduction and planning. A wide variety of indices have been developed to quantify fire risk, recently reviewed by de Groot et al. (2015). Although they are usually tuned to specific regions, some have been used successfully in global-scale climate simulations (e.g. Betts et al., 2015, Burton et al., 2018), including the two we consider here: the McArthur index and the Angström index.

The McArthur Forest Fire Danger Index Mark 5 was first developed for Australia, and is calculated on a daily basis, integrating information on past rainfall leading up to each day (Noble et al., 1980):

$$I_{\mathrm{M}} = 1.275 f_{\mathrm{drt}}^{0.987} \exp\left(\frac{T_{\mathrm{C,max}}}{T_{\mathrm{M0}}} - \frac{\mathrm{RH}_{\%,\mathrm{min}}}{\mathrm{RH}_{\mathrm{M0}}} + \frac{W}{W_{\mathrm{M0}}}\right), \tag{1}$$

where $T_{\mathrm{C,max}}$ is the maximum daily temperature in °C, $\mathrm{RH}_{\%,\mathrm{min}}$ is the daily minimum relative humidity as a percentage and W is the daily mean wind speed in $\mathrm{m\,s^{-1}}$. The scale constants are $T_{\mathrm{M0}} = 29.5858\,^{\circ}\mathrm{C}$, $\mathrm{RH}_{\mathrm{M0}} = 28.9855\,\%$, and $W_{\mathrm{M0}} = (42.735/3.6)\,\mathrm{m\,s^{-1}}$. The Keetch and Byram (1968) drought index f_{drt} has a maximum limit of 10 (Sirakoff, 1985), and is given by

$$f_{\mathrm{drt}} = \min\left[0.191\,(a_{\mathrm{restore}} + 104)\,\frac{(N+1)^{1.5}}{3.52(N+1)^{1.5} + R - 1}, 10\right] \tag{2}$$

where N is the number of days since the last day with rainfall, and R is the amount of rainfall on that day in mm.

The restore amount, a_{restore}, is the amount of water needed to restore the water content of the soil to field capacity, given in the range 0–200 mm. Given the difficulty in obtaining global soil moisture observations, we remove the soil moisture dependence entirely, by setting a_{restore} to a constant value of 120 mm, as used in Golding and Betts (2008). We have tested the effect of this simplification on correlations of seasonal means in Appendix A.

The McArthur fire index is used particularly in Australia, South Africa and Spain (de Groot et al., 2015), but it has also been shown to strongly correlate with satellite estimates of actual fire occurrence in the Amazon (Hoffmann et al., 2003), and Golding and Betts (2008) used it in their study of Amazonian fire risk under future climates. Note that the McArthur index is defined such that higher values indicate greater risk.

The Angström index has a much simpler definition:

$$I_{\mathrm{A}} = \frac{\mathrm{RH}_{\%}}{\mathrm{RH}_{\mathrm{A0}}} + \frac{T_{\mathrm{A1}} - T_{\mathrm{C}}}{T_{\mathrm{A0}}}, \tag{3}$$

where $RH_{\%}$ is daily mean relative humidity as a percentage, and T_C is the daily mean temperature in °C. The scale constants are $RH_{A0} = 20\,\%$, $T_{A0} = 10\,°C$ and $T_{A1} = 29\,°C$, following Eastaugh et al. (2012); other constants are also in use, e.g. Skvarenina et al. (2004) and Holsten et al. (2013). Since this equation is linear, it can also be used with monthly or seasonal mean relative humidity and temperature values. Note that smaller values of the Angström index indicate greater fire risk.

The Angström index was developed in the first half of the Twentieth Century in Sweden, and has been used throughout the Scandinavian Peninsula (Hamadeh et al., 2017), but has had success in other countries such as Slovakia (Skvarenina et al., 2004), Taiwan (Lin, 1995), Germany (Holsten et al., 2013), Austria (Arpaci et al., 2013) and Brazil (Alves White et al., 2013).

We calculate reference values of both fire indices, using the observation-based WFDEI reanalysis data set (*WATCH Forcing Data methodology applied to ERA-Interim*, Weedon et al. 2011, 2014, using CRU precipitation). This covers land points only, on a 0.5° grid. We calculate the reference Angström index from monthly mean temperature and relative humidity. We calculate the reference McArthur index using daily maximum temperature, daily minimum relative humidity, daily mean windspeed, and daily precipitation. We use a near-zero threshold for daily precipitation (10^{-8} mm), but we have also tested a higher level (5 mm) following Keetch and Byram (1968). The seasonal-mean results from using either threshold using the WFDEI data are very highly correlated.

Although these fire indices do not account for available fuel in their quantification of fire risk, we mask out gridcells where the fraction of bare soil is ≥ 0.5, following Gilham (2014). This removes regions without substantial amounts of vegetation to burn.

It is important to understand how the fire risk indices we consider here relate to actual fire occurrence. In principle, there could be significant differences: the fire indices do not explicitly account for fuel availability or chance of ignition, for example. These indices are based solely on meteorological factors, as opposed to human factors. We use observations of burnt area to quantify fire occurrence, using v4.1s of the Global Fire Emissions Database (GFED, Giglio et al. 2013, Randerson et al. 2017), which includes an experimental adjustment for small fires (Randerson et al., 2012, van der Werf et al., 2017). The GFED data starts in 1997, later than the other data sets we use.

2.2. Net Primary Productivity

Net primary productivity is calculated from the carbon assimilated from photosynthesis minus the carbon lost by respiration. This quantity is not directly observable. At the site level, eddy correlation techniques can be used to measure net ecosystem exchange, which incorporates both NPP and soil respiration. Field-based measurements can give accurate NPP data on a small scale, but it is difficult to estimate NPP on larger scales due to sparse observation networks (Pachavo and Murwira, 2014). Satellite products exist (e.g. MODIS NPP, Zhao et al. 2006, Heinsch et al. 2006), but these are themselves based on models, and they can be contaminated by cloud cover – particularly relevant in the Tropics. The MODIS NPP data is only available from 2000, which would give too short a period to assess the skill of seasonal forecasts.

To avoid these problems, and for greater internal consistency, we calculate the

reference values of NPP using JULES, driven by the WFDEI reanalysis data. In JULES, NPP depends strongly on soil moisture (Clark et al. 2011, Harper et al. in prep). Soil moisture depends on evaporation and transpiration, which in turn depend on vegetation cover and atmospheric conditions (in particular, temperature and humidity, with wind also being a factor). NPP in JULES also has a strong dependence on temperature (Clark et al., 2011), via both photosynthesis and respiration.

Modelled primary productivity in JULES has been evaluated against a number of observational datasets, and is shown to successfully reproduce interannual variability of GPP on global scales, while on a regional scale GPP in the tropics was biased to higher values than observed (Slevin et al., 2017).

Our JULES simulations are driven by WFDEI reanalysis data, as described above. The JULES configuration used is based on 'JULES-C' as used in the Global Carbon Budget annual assessments (Le Quéré et al., 2018) and assessed for its ENSO response characteristics (Bastos et al., 2018). In the application here the dynamic vegetation model was switched off and the vegetation cover prescribed using the International Geosphere and Biosphere Programme (IGBP) land classification dataset, processed as part of the WFDEI project. The vegetation and soil ancillary was generated by the Central Ancillary Program (Dharssi et al., 2009) on the WFDEI grid, using the Brooks and Corey (1964) parameterisation. The topographic index data was from Hydro1k (EROS Archive, 2017). The model was forced with global CO_2 from NOAA.‡

2.3. Seasonal forecasts

We use data from the GloSea5 seasonal forecast system (MacLachlan et al., 2015) in its Global Coupled 2.0 (GC2) configuration, based on the Hadley Centre General Environment Model version 3 (HadGEM3-GC2, Williams et al., 2015). This coupled climate model uses an atmospheric grid of 0.83° longitude by 0.55° latitude, with a well-resolved stratosphere and a 0.25° ocean grid. The land surface model component is the GL6.0 configuration of JULES (Best et al., 2011, Walters et al., 2017). We use a hindcast data set comprising 24-member ensemble forecasts of the December–January–February (DJF) and June–July–August (JJA) seasons each year, initialised around 1st November and 1st May respectively. The hindcasts are produced for the 20 years of 1992–2011 for the JJAs and 1992/93 to 2011/12 for the DJFs. Soil moisture is initialised using JULES driven by the WFDEI reanalysis. While the skill of different GloSea5 outputs has been evaluated in a variety of different contexts and applications, of particular relevance here is that GloSea5 has very high levels of skill in forecasting ENSO (MacLachlan et al., 2015), and in forecasting rainfall in the tropics (Scaife et al., 2017, 2019). Note that the version of JULES used within GloSea5 is less recent than the one we use to calculate observation-based NPP (see previous subsection).

Calculating the Angström fire index from the hindcast data is reasonably straightforward. As already discussed, the Angström index is linear, so its seasonal mean values can be calculated directly from monthly mean forecast output. In contrast, the McArthur index can only be approximated by the forecast data. Although daily maximum temperature and daily mean wind speed were available, the daily minimum relative humidity was not stored when the forecasts were made, so we have used the daily mean in that case. A second difficulty is in the calculation of the drought factor: the number of days since there has been any rainfall could be

‡ `https://data.giss.nasa.gov/modelforce/ghgases/Fig1A.ext.txt`, downloaded from `https://data.giss.nasa.gov/modelforce/ghgases/`, based on Hansen et al. (2007).

longer than the forecast lead time in some locations (e.g. before 25th Oct, 1st Nov or 9th Nov for the DJF forecasts). Those cases are masked out of our calculations.

To make an initial assessment of the forecast skill, we will be using the simple interannual Pearson correlation between the seasonal mean, ensemble mean hindcast data, and the reference data derived from observations. Using the ensemble mean ensures that we are maximising the predictable signal from the ensemble; having skill in the ensemble mean is a necessary first step before examining more complex skill metrics based on the distribution of ensemble members.

We are not applying any bias correction to any of the hindcast data. While the Pearson correlation is not sensitive to overall seasonal-mean biases, the fact that there are many absolute thresholds in the fire index definitions means that model biases could still affect the results. We are also not detrending any of the data when assessing its skill. While it is often informative to understand how much of a skillful forecast comes from a trend versus other processes, in our case it is just as relevant to know that the model is able to reproduce an observed trend. Studies detailing the ability of a seasonal forecast to produce a useful climate service for a particular user would require more detailed consideration of biases and trends, as well as probabilistic skill assessment. For this initial study, of how well the initialised climate model on its own can capture the processes necessary for forecasting relevant components of the carbon cycle, we simply test the correlation.

3. Results

We first show how tropical NPP and fire risk behave under El Niño and La Niña conditions in our observation-based data sets. This provides important context for the subsequent subsections on their performance within the GloSea5 hindcasts. For consistency, all plots cover the same 20-year period as the hindcast (1992/93–2011/12), unless noted otherwise.

Figure 1(a) shows, for meteorological context, the mean anomalies of seasonal rainfall totals under El Niño and La Niña conditions, based on the Oceanic Niño Index§ (ONI): A season is labelled as being El Niño if its seasonal mean value is $> 0.5\,\mathrm{K}$; and as La Niña if its ONI $< -0.5\,\mathrm{K}$. We classify DJFs and JJAs separately according to their own ONI values. There are clear regions of enhanced or reduced precipitation across the Tropics, with impacts in different regions at different times of the year.

3.1. NPP and fire index relationship with El Niño

Figure 1(b) shows the response of NPP to Niño and La Niña events in DJF and JJA. There are regions of both reduced and enhanced productivity in each case. The response matches that of precipitation in northern South America in DJF, and in Africa in both seasons. However, there is an additional signal in NPP in northeastern Brazil in JJA, and NPP does not reflect the clear precipitation response in Indonesia in JJA.

Similar composite maps are shown for the McArthur and Angström fire indices in figures 1(c) and (d). These follow the precipitation response more closely, with enhanced fire risk in northern South America, southern Africa and northwestern

§ https://origin.cpc.ncep.noaa.gov/products/analysis_monitoring/ensostuff/ONI_v5.php

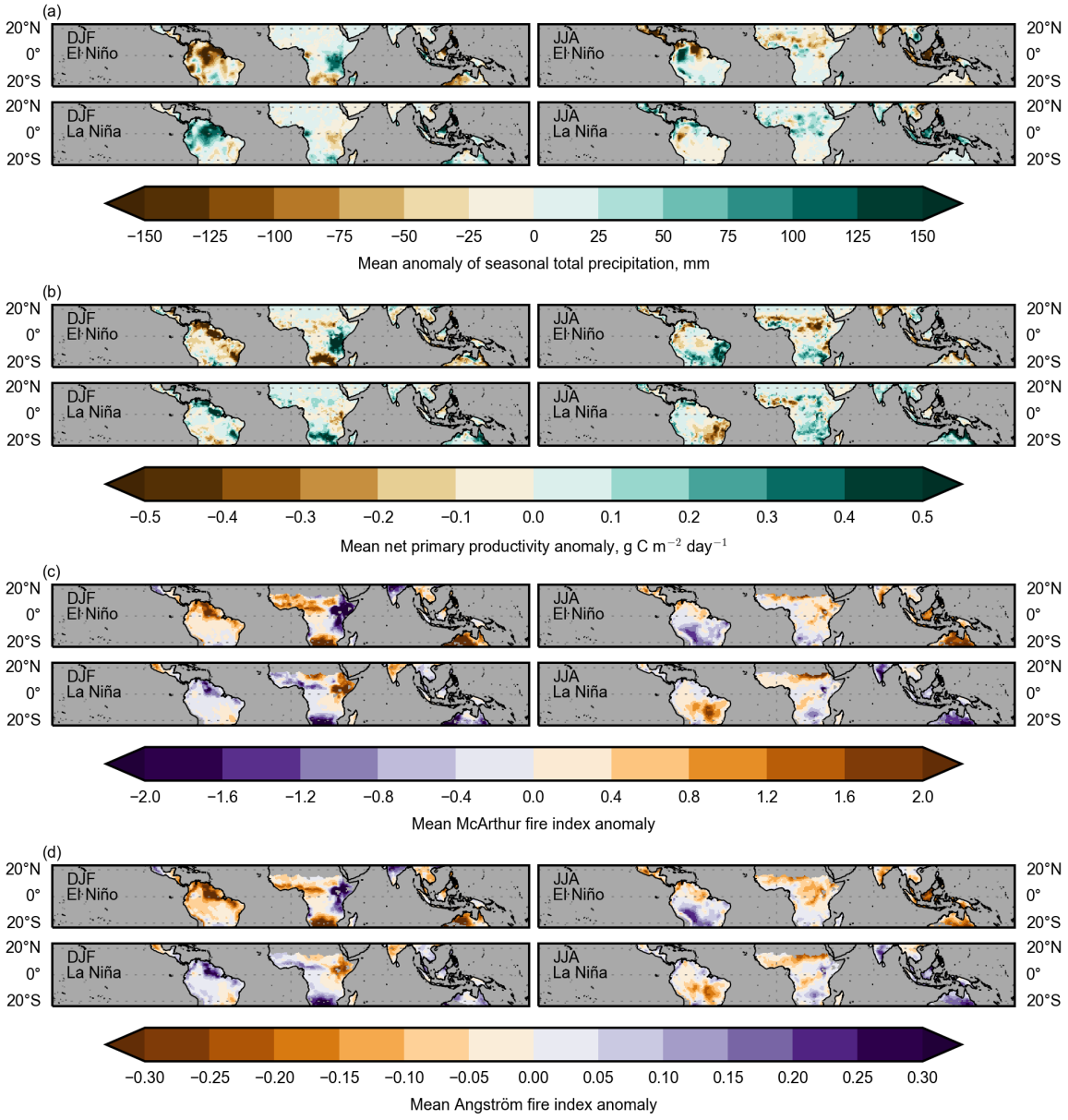

Figure 1. Each set of 4 panels shows the mean anomalies of observation-based data for a given quantity for El Niño and La Niña DJF and JJA seasons, with respect to the climatology for that season. (a) WFDEI precipitation. (b) NPP from WFDEI-driven JULES runs. (c) McArthur fire index calculated from WFDEI data. (d) Angström fire index calculated from WFDEI data. Note that the colour scheme has been switched in this case to be consistent with orange indicating greater fire risk. DJF climatologies are calculated for the 1992/93–2011/12 period, and JJA climatologies for the 1992–2011 period.

Australia in DJF El Niños, and in Indonesia and eastern India in JJA El Niños. As with NPP, there are some additional responses, such as the Sahel, the Horn of Africa, and India in DJF, and northern Australia in JJA.

3.2. Fire index relationship with burnt area

Figure 2(a) shows the ENSO response in the observed burnt area data. For consistency with our other results, we only use the period up to the end of the GloSea5 hindcast data set, i.e. the 15 years of 1997/98 to 2011/12 for DJF, and 1997–2011 for JJA. As the GFED data set is based on very high resolution observations of individual fires, this data is much more spatially varied than the meteorology-based data shown previously (all our figures use data regridded to match the GloSea5 data). Nevertheless, there are clear similarities with the fire risk indices, particularly in northern South America, the Sahel and northwest Australia in DJF. It is important to note that the two seasons we focus on here do not necessarily correspond to the peak fire seasons around the world; for completeness, we show the burnt area ENSO response in the other two seasons, and the climatology in all four seasons, in Appendix B.

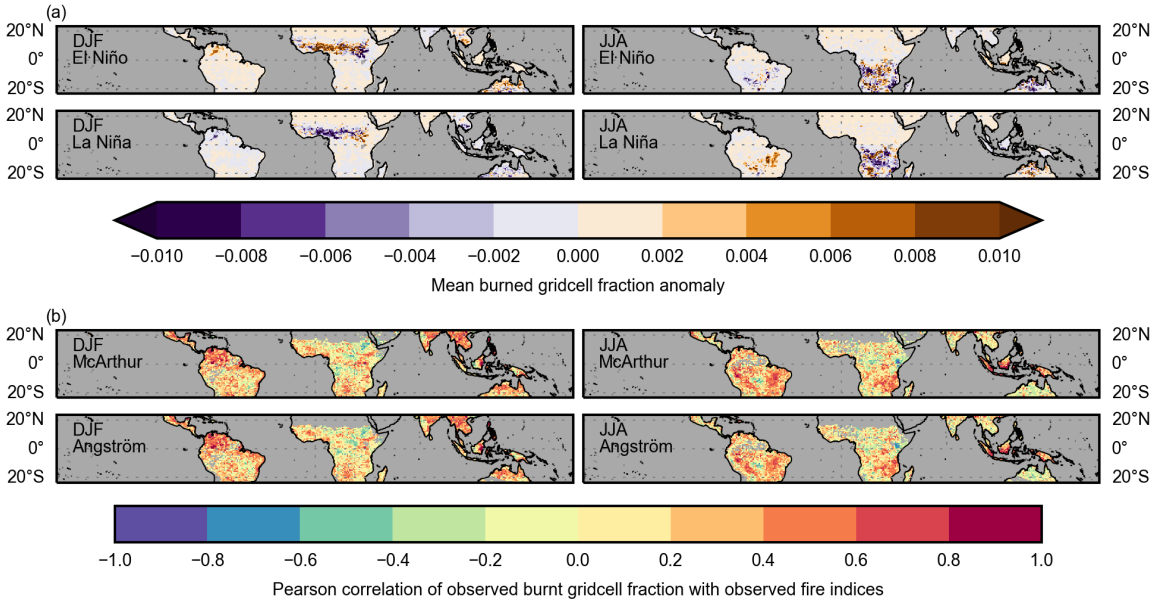

Figure 2. (a) Mean anomalies of GFED burnt area in El Niño and La Niña DJF and JJA seasons with respect to the climatology for that season. DJF climatologies are calculated for the 1997/98–2011/12 period, and JJA climatologies for the 1997–2011 period. (b) Correlation between GFED burnt area and observation-based McArthur fire index (top) and Angström fire index (bottom), for DJF (left) and JJA (right). The correlations with the Angström index have had their sign switched, to aid comparison. Significance contours are not drawn, but a Fisher z-test for the 15 years of data here would indicate that a correlation would have to be $|r| > 0.51$ to be significantly different to zero at the 5% level.

To clarify the relationship between burnt area and the fire risk indices, figure 2(b) maps the correlation of their seasonal mean time series. This shows that, in almost all

the regions where the fire indices respond strongly to ENSO, they are well correlated with observed burnt area, although a noticeable exception is northern Australia in JJA. This gives us confidence that the fire indices give a reasonable estimate of fire risk.

However, one of the most important features seen in figure 1(c), (d) and figure 2 is that there is very little difference between the results for the McArthur and Angström fire indices: they both perform equally well/poorly in terms of following the interannual variability of burnt areas in the tropics. This is backed up by plotting the correlation between the two fire indices themselves (figure 3): they are very highly (anti-)correlated, with values $r < -0.8$ in most places for both seasons, over the 20-year period we consider here. The additional complexity in modelling fire risk that goes into the McArthur index does not seem important for most regions of the tropics for forecasting seasonal means.

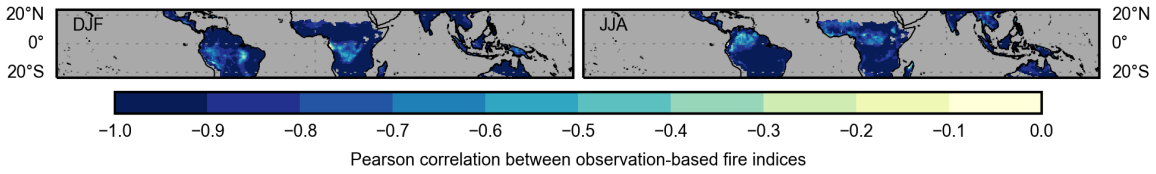

Figure 3. Correlation between the observation-based values of the McArthur and Angström fire indices, for DJF (left) and JJA (right). This covers the same 20 year periods as the GloSea5 hindcast; a correlation must be $|r| > 0.44$ to be significantly different to zero according to a Fisher z-test at the 5% level, and this test is passed almost everywhere.

3.3. Seasonal forecasting skill

In the following figures, we show skill maps of seasonal forecasts. Figure 4 shows this measure of forecast skill for NPP, and figure 5 shows the skill for the McArthur and Angström fire indices. Figure 6 shows the skill of their underpinning meteorological variables: temperature, precipitation, relative humidity and wind speed.

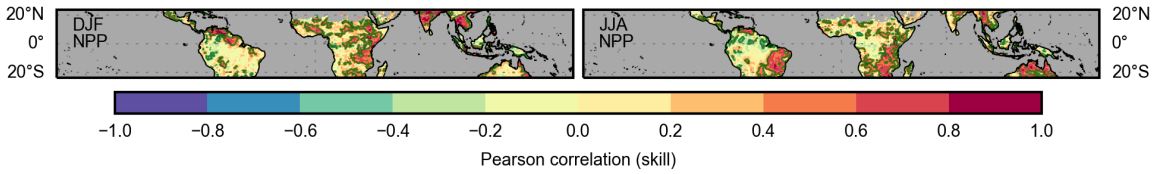

Figure 4. Correlation between ensemble-mean data from the GloSea5 hindcast, and observation-based data for NPP, for DJF (left) and JJA (right). A green contour marks $|r| = 0.44$; correlations larger than this are significantly different to zero at the 5% level, based on a Fisher z-test.

3.3.1. NPP and its components. In DJF, there is skill in NPP forecasts (figure 4) in equatorial South America, Africa, India and the Indochinese Peninsula. However, air temperature, precipitation, relative humidity and wind speed all show greater skill

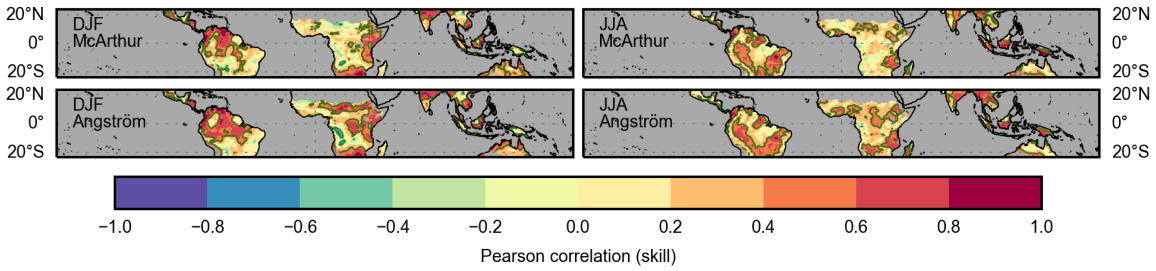

Figure 5. As figure 4, but showing the correlation skill for the McArthur fire index (top) and Angström fire index (bottom). The green contour marks significance at the 5% level based on a Fisher z-test.

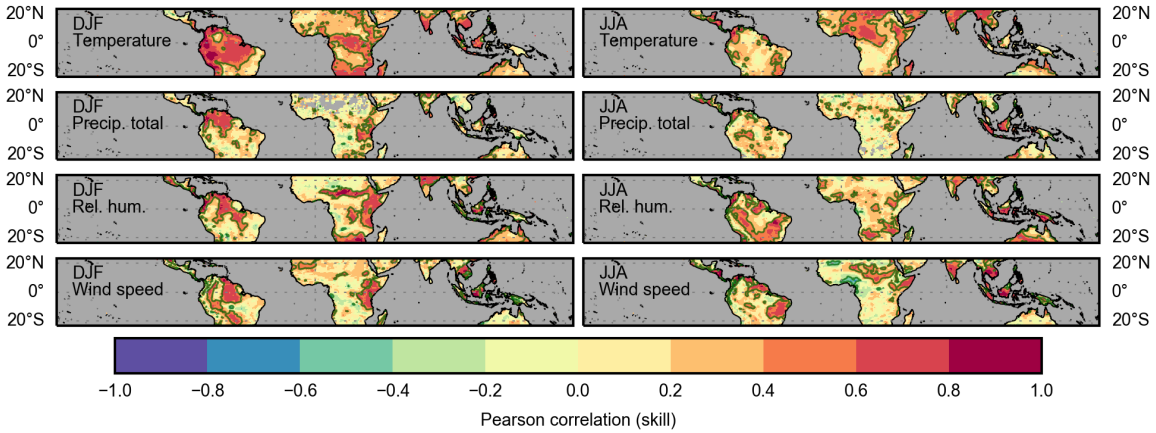

Figure 6. As figure 4, but showing the correlation skill for the meteorological variables, as labelled. The green contour marks significance at the 5% level based on a Fisher z-test.

over much larger areas of South America in DJF (figure 6), particularly in the region from the Venezuelan coast south to the Amazon river. This is a good demonstration of how skill in the underlying variables does not map directly on to skill in the compound variables. In India and Indochina, the high correlation in NPP seems more related to temperature, with Indochina in particular not showing widespread skill in relative humidity or precipitation. These are also regions that do not show a clear ENSO response in DJF.

In JJA, the correlation between reanalysis-forced NPP and GloSea NPP is high in northern Venezuela, northeastern Brazil, eastern Africa and northern Australia. These regions show a strong response to El Niño in JJA (figure 1b), related to precipitation (figure 1a): reduced productivity in areas that get drier during an El Niño (Venezuela, Australia), and increasing in areas that get wetter (northeast Brazil).

The NPP skill shown could have useful applications, such as for agricultural production in northeast Brazil. In this region, the main contributor to the high skill is likely to be the depletion in soil moisture due to evapotranspiration, affected by relative humidity and wind speed, which both show skill in this area.

3.3.2. Fire indices and their components. There are large areas of skill in both DJF and JJA for the McArthur fire index, with very similar patterns seen for the Angström index skill (figure 5). The areas of skill largely correspond to where the fire indices in these seasons respond strongly to ENSO (figures 1c and d). Comparing with the skill of the meteorological variables (figure 6), it is clear that the skill patterns are very similar to those of relative humidity and (to a lesser extent) wind speed and precipitation. The temperature skill patterns differ, but temperature is more skillful generally, over broader areas, partly from the trend.

Finally, we estimate the skill in forecasting burnt area from GloSea5, using fire indices and a single meteorological variable as linear predictors (i.e. simply the correlation between a variable from the GloSea5 hindcast and the observation-based burnt area data). Figure 7 shows the Pearson correlation for each of these variables with burnt area. Here, a strong positive or negative correlation indicates that the variable could be used as a skillful predictor.

Although the skill is clearly reduced compared to forecasting the fire indices or meteorological variables themselves, there are nevertheless some coherent large-scale regions that suggest useful levels of skill: northern South America, southern Indochinese Peninsula, northwestern Australia in DJF; northeastern Brazil, east Africa and Indonesia in JJA. It also appears that, to a large extent, just using a single meteorological variable could provide skillful forecasts of fire risk in some regions.

As expected from our examination of the observation-based data, the additional complexity of the McArthur index does not significantly improve the forecast skill, either of the fire indices themselves, or of actual burnt area.

4. Discussion and conclusions

This study has examined the seasonal forecasting skill of two key processes that contribute to the interannual variability of global CO_2 levels: fire risk and net primary productivity. While we expect that hybrid dynamical–statistical forecasts (e.g. based on ENSO, similar to Betts et al. 2016, 2018) will still be the best approach to forecasting global CO_2, our investigation is useful for highlighting underlying capabilities in the climate model used for our seasonal forecasts. We highlight where the forecasts do and do not have skill, in different regions and at different times of the year, in order to determine whether the skill is in the key regions and seasons that contribute to the CO_2 variability. The regional distribution of skill can also inform approaches to seasonal forecasting, and, in principle, the development of climate services for agriculture and fire risk management.

The seasonal forecast skill for the NPP modelled explicitly in GloSea5 is significant for large areas of the Tropics, including where NPP responds strongly to ENSO. Some of the regions where it is skillful are well-placed for forecasting crop yield, such as northeast Brazil.

The fire indices we have considered also show significant skill across much of the Tropics. However, we have also demonstrated, in observations as well as in terms of seasonal forecast skill, that on seasonal-mean time scales there is no benefit to using the detailed McArthur fire index over a simple indicator of hot and dry conditions – the Angström fire index. Any benefits from having a more detailed, carefully-calibrated fire index, as might be seen on weather-forecasting time scales, are lost when averaging over a season. The resulting skill picks out large-scale features in common across both indices: areas where it becomes anomalously dry and hot at similar times. We have

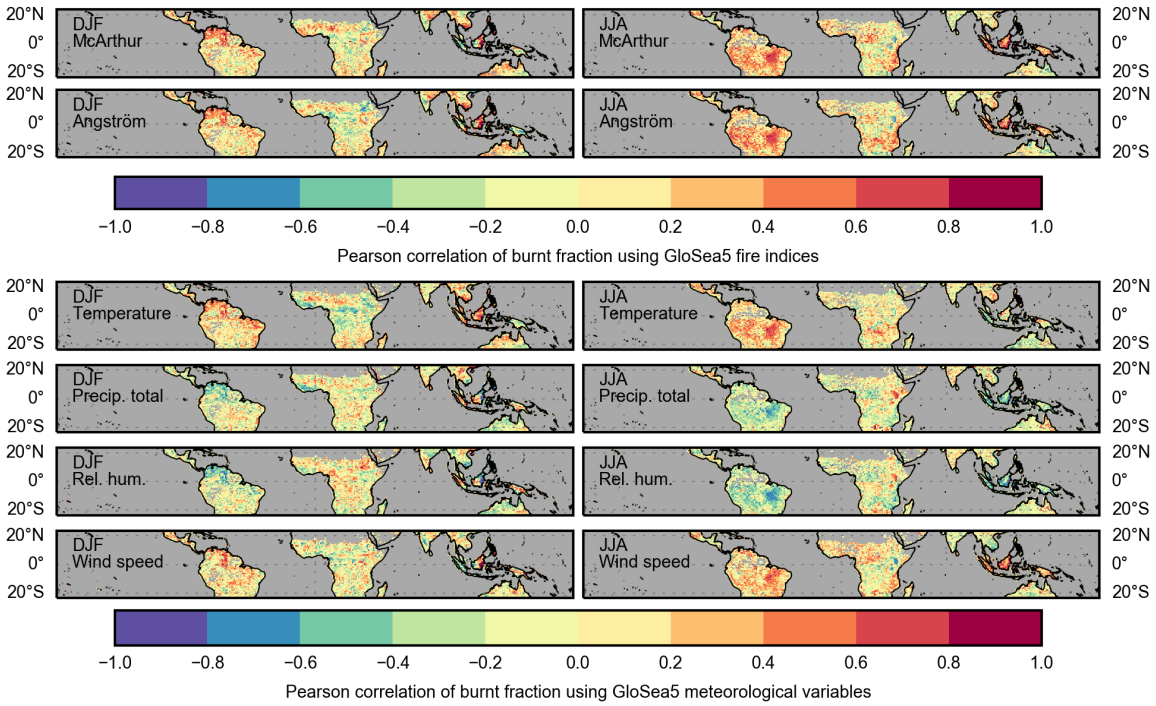

Figure 7. Correlation between the observed burnt fractions using the ensemble-mean fire indices and meteorological variables (as labelled) from the GloSea5 hindcast. The correlation for the Angström index has had its sign switched, for consistency with the McArthur index. Significance contours are not drawn, but as this only uses 15 years of data, a nominal threshold for significance at the 5% level would be $|r| > 0.51$.

demonstrated that there are several regions where burnt area itself could be forecast skilfully, based either on a fire risk index, or perhaps even on a single meteorological variable.

A third process that is not considered here, but which is also an important contributor to the interannual variability of terrestrial carbon emissions is heterotrophic respiration. This is currently modelled within the GloSea5 system but not available as an output variable. Model heterotrophic respiration includes a factor that depends explicitly on soil temperature and a factor that depends explicitly on soil moisture (Clark et al., 2011). An interesting extension to this work would be to look whether the GloSea5 system can skilfully predict these two factors, and how much of this skill can be captured for season means using a simple combination of meteorological variables such as air temperature, precipitation and wind speed.

Our results are a clear demonstration of the different kinds of analysis required when considering seasonal climate prediction, compared to weather forecasting studies, which require confidence at forecasting individual fire events; or climate projection timescales, where longer-term feedbacks are crucial. When forecasting seasonal means, simplicity is important. An impacts model that requires driving data from many input variables, at high temporal resolution, is unlikely to result in any benefit in terms of

skill; much simpler metrics based on one or two variables on monthly-to-seasonal timescales are likely to be a more efficient way of achieving skillful forecasts. (Palin et al. 2016 and Bett et al. 2019 have demonstrated this point in the very different contexts of seasonal forecasting for transport and energy sector impacts in Europe.)

This also applies to interactive models, like JULES' fire model INFERNO (Mangeon et al., 2016, Burton et al., 2019): While INFERNO adds value at climate projection timescales, where feedbacks between atmospheric CO_2 and vegetation distributions are important, it is unlikely that including INFERNO in the GloSea system would give increased skill at forecasting burnt area at seasonal timescales, given the current level of skill of the relevant meteorological variables.

Development of climate services, for crop yield or fire risk, would require more detailed assessments, considering bias correction and probabilistic forecast calibration, similar to the study by Bedia et al. (2018) on seasonal forecasting fire risk in the Mediterranean. While they used the Canadian Fire Weather Index, similar in complexity to the McArthur index used here, they also found that their regions of good skill were closely linked to skill in forecasting relative humidity. Being able to use simpler impacts metrics could greatly simplify the development and production of seasonal climate services for forecasting fire risk. However, it could be the case that, operationally, the most important quantity to forecast is not the seasonal mean, but rather the number of high fire risk days within the season. This should be determined in conjunction with the relevant stakeholder as part of the co-development of the forecast service.

Our study is intended to be a starting point for investigating model capability for seasonal forecasting of carbon cycle components. There are of course many limitations: The NPP reference data are reanalysis-driven model runs; it was necessary to approximate the fire index calculations due to limitations in available data; and the number of years in the hindcast results in large uncertainties in the correlation skill. However, we have demonstrated that GloSea5 has significant skill in forecasting the year-to-year variation in NPP and fire risk, which are important components in the carbon cycle processes that contribute towards global CO_2 variability.

Acknowledgments

The authors wish to thank Richard Betts for discussing his work on CO_2 forecasting with us prior to publication, and Inika Taylor for useful discussions regarding simplifications of the Keetch and Byram drought index. The Hydro1k topographic index data was formatted by Doug Clark and Graham Weedon. CAP was run by Kier Bovis and Heather Ashton. We thank Penny Boorman for providing MODIS files in netCDF format. CB and AW were supported by the Newton Fund through the Met Office Climate Science for Service Partnership Brazil (CSSP Brazil). AS was supported by the UK-China Research & Innovation Partnership Fund through the Met Office Climate Science for Service Partnership (CSSP) China as part of the Newton Fund.

Appendix A. Soil moisture dependence of McArthur fire index

Throughout this paper we have used a simplified McArthur fire index, based on the McArthur Forest Fire Danger Index Mark 5, but with a constant restore amount a_{restore} in the drought factor (equation 2). We have tested using an explicit soil

moisture (θ) dependence by calculating a_{restore} as the amount of water needed to restore the top 1 m of soil to field capacity (θ_{FC}, at -0.01 MPa), as a fraction of the difference between field capacity and soil moisture wilting point (θ_{W}, at -1.5 MPa), rescaled to be in the interval 0–200 mm:

$$a_{\text{restore}} = \begin{cases} 0 & \text{for } \theta \geq \theta_{\text{FC}} \\ 200\left(\dfrac{\theta_{\text{FC}} - \theta}{\theta_{\text{FC}} - \theta_{\text{W}}}\right) & \text{for } \theta_{\text{W}} < \theta < \theta_{\text{FC}} \\ 200 & \text{for } \theta \leq \theta_{\text{W}} \end{cases} \tag{A.1}$$

This formulation has been informed by Holgate et al. (2017) and Walsh et al. (2017).

We used the daily soil moisture from the same WFDEI-driven JULES simulations we ran for our reference NPP calculations, to calculate a new McArthur fire index data set for testing.

Despite the restore amount showing significant regional variation (figure A1), the seasonal mean McArthur index based on varying soil moisture, and the simplified index using a constant restore amount, are very highly correlated (figure A2).

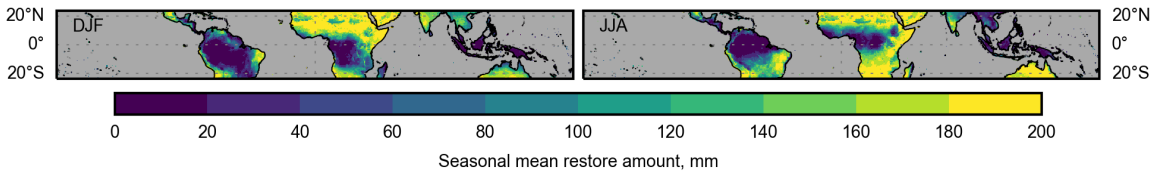

Figure A1. Climatological mean values of the restore amount, calculated using the method outlined in the appendix.

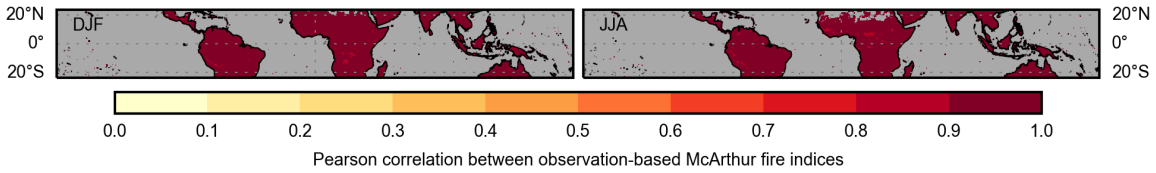

Figure A2. Correlation between the observation-based values of the McArthur fire index using a soil moisture-dependent restore amount, and a constant restore amount, for DJF (left) and JJA (right).

Appendix B. Burnt area seasonal climatologies throughout the year

Figure B1 shows the climatological seasonal mean fields for burnt fraction of gridcells, covering all four seasons: DJF and JJA as in the body of this paper, plus March–April–May (MAM) and September–October–November (SON). This illustrates the regional distribution of the peak fire season throughout the year.

Figure B2 shows, for completeness, the response of the burnt fractions to ENSO, as in figure 2(a), but for MAM and SON.

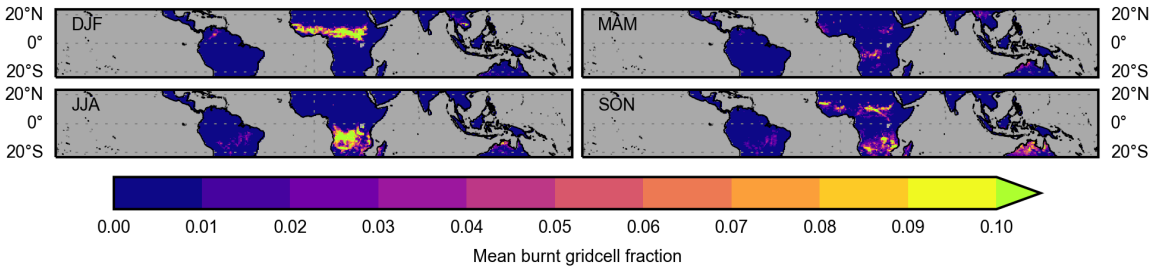

Figure B1. Maps of the climatological seasonal mean values of burnt fraction of grid cells, for all four seasons as labelled. As with other burnt area figures, we use the 15 years from 1997/98–2011/12.

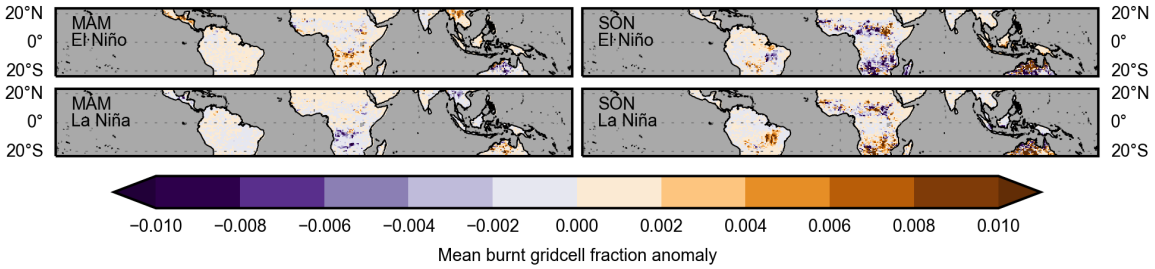

Figure B2. As Figure 2(a), but for the other seasons, MAM and SON, as labelled.

References

Alves White, B. L., Secundo White, L. A., Ribeiro, G. T., and Martins Fernandes, P. A. Development of a fire danger index for eucalypt plantations in the northern coast of Bahia, Brazil. *Revista Floresta*, 43(4):601–610, December 2013. doi:10.5380/rf.v43i4.30973.

Aragao, L., Anderson, L., Fonseca, M., Rosan, T., Vedovato, L., Wagner, F., Silva, C., Silva, C., Arai, E., Aguiar, A., Barlow, J., Berenguer, E., Deeter, M., Domingues, L., Gatti, L., Gloor, M., Malhi, Y., Marengo, J., Miller, J., Phillips, O., and Saatchi, S. 21st century drought-related fires counteract the decline of Amazon deforestation carbon emissions. *Nat. Commun.*, 9(536), 2018. doi:10.1038/s41467-017-02771-y.

Arpaci, A., Eastaugh, C. S., and Vacik, H. Selecting the best performing fire weather indices for Austrian ecoregions. *Theor. Appl. Climatol.*, 114(3):393–406, November 2013. doi:10.1007/s00704-013-0839-7.

Barnston, A. G., Tippett, M. K., L'Heureux, M. L., Li, S., and DeWitt, D. G. Skill of real-time seasonal ENSO model predictions during 2002–11: Is our capability increasing? *Bulletin of the American Meteorological Society*, 93(5):631–651, 2012. doi:10.1175/BAMS-D-11-00111.1.

Bastos, A., Friedlingstein, P., Sitch, S., Chen, C., Mialon, A., Wigneron, J.-P., Arora, V. K., Briggs, P. R., Canadell, J. G., Ciais, P., Chevallier, F., Cheng, L., Delire, C., Haverd, V., Jain, A. K., Joos, F., Kato, E., Lienert, S., Lombardozzi, D., Melton, J. R., Myneni, R., Nabel, J. E. M. S., Pongratz, J., Poulter, B., Rödenbeck, C.,

Séférian, R., Tian, H., van Eck, C., Viovy, N., Vuichard, N., Walker, A. P., Wiltshire, A., Yang, J., Zaehle, S., Zeng, N., and Zhu, D. Impact of the 2015/2016 el niño on the terrestrial carbon cycle constrained by bottom-up and top-down approaches. *Philosophical Transactions of the Royal Society B: Biological Sciences*, 373(1760): 20170304, 2018. doi:10.1098/rstb.2017.0304.

Bedia, J., Golding, N., Casanueva, A., Iturbide, M., Buontempo, C., and Gutiérrez, J. M. Seasonal predictions of Fire Weather Index: Paving the way for their operational applicability in Mediterranean Europe. *Clim. Serv.*, 9:101–110, January 2018. doi:10.1016/j.cliser.2017.04.001.

Best, M. J., Pryor, M., Clark, D. B., Rooney, G. G., Essery, Ménard, C. B., Edwards, J. M., Hendry, M. A., Porson, A., Gedney, N., Mercado, L. M., Sitch, S., Blyth, E., Boucher, O., Cox, P. M., Grimmond, C. S. B., and Harding, R. J. The joint UK land environment simulator (JULES), model description – part 1: Energy and water fluxes. *Geosci. Model Dev.*, 4(3):677–699, September 2011. doi:10.5194/gmd-4-677-2011.

Bett, P., Thornton, H. E., Troccoli, A., De Felice, M., Suckling, E., Dubus, L., Saint-Drenan, Y.-M., and Brayshaw, D. J. A simplified seasonal forecasting strategy, applied to wind and solar power in Europe. *EarthArXiv*, Apr 2019. doi:10.31223/osf.io/kzwqx.

Betts, R. A., Golding, N., Gonzalez, P., Gornall, J., Kahana, R., Kay, G., Mitchell, L., and Wiltshire, A. Climate and land use change impacts on global terrestrial ecosystems and river flows in the HadGEM2-ES Earth system model using the representative concentration pathways. *Biogeosciences*, 12(5):1317–1338, 2015. doi:10.5194/bg-12-1317-2015.

Betts, R. A., Jones, C. D., Knight, J. R., Keeling, R. F., and Kennedy, J. J. El Niño and a record CO_2 rise. *Nature Climate Change*, 6(9):806–810, June 2016. doi:10.1038/nclimate3063.

Betts, R. A., Jones, C. D., Knight, J. R., Keeling, R. F., Kennedy, J. J., Wiltshire, A. J., Andrew, R. M., and Aragão, L. E. O. C. A successful prediction of the record CO_2 rise associated with the 2015/2016 El Niño. *Philosophical Transactions of the Royal Society of London B: Biological Sciences*, 373(1760), 2018. doi:10.1098/rstb.2017.0301.

Brooks, R. H. and Corey, A. T. Hydraulic properties of porous media. Hydrology Papers 3, Colorado State University, March 1964. URL `http://hdl.handle.net/10217/61288`.

Burton, C., Betts, R. A., Jones, C. D., and Williams, K. Will fire danger be reduced by using solar radiation management to limit global warming to 1.5°C compared to 2.0°C? *Geophys. Res. Lett.*, 45(8):3644–3652, 2018. doi:10.1002/2018GL077848.

Burton, C., Betts, R., Cardoso, M., Feldpausch, T. R., Harper, A., Jones, C. D., Kelley, D. I., Robertson, E., and Wiltshire, A. Representation of fire, land-use change and vegetation dynamics in the Joint UK Land Environment Simulator vn4.9 (JULES). *Geosci. Model Dev.*, 12(1):179–193, 2019. doi:10.5194/gmd-12-179-2019.

Chen, Y., Randerson, J. T., Morton, D. C., DeFries, R. S., Collatz, G. J., Kasibhatla, P. S., Giglio, L., Jin, Y., and Marlier, M. E. Forecasting fire season severity in South America using sea surface temperature anomalies. *Science*, 334(6057):787–791, November 2011. doi:10.1126/science.1209472.

Chen, Y., Morton, D., Andela, N., van der Werf, G., Giglio, L., and Randerson, J. A pan-tropical cascade of fire driven by El Niño Southern Oscillation. *Nature Climate Change*, 7(12):906–911, 2017. doi:10.1038/s41558-017-0014-8.

Chen, Y., Morton, D. C., Andela, N., Giglio, L., and Randerson, J. T. How much global burned area can be forecast on seasonal time scales using sea surface temperatures? *Environ. Res. Lett.*, 11(4):045001, April 2016. doi:10.1088/1748-9326/11/4/045001.

Clark, D. B., Mercado, L. M., Sitch, S., Jones, C. D., Gedney, N., Best, M. J., Pryor, M., Rooney, G. G., Essery, R. L. H., Blyth, E., Boucher, O., Harding, R. J., Huntingford, C., and Cox, P. M. The Joint UK Land Environment Simulator (JULES), model description – Part 2: Carbon fluxes and vegetation dynamics. *Geosci. Model Dev.*, 4(3):701–722, 2011. doi:10.5194/gmd-4-701-2011.

Clark, R. T., Bett, P., Thornton, H., and Scaife, A. Skilful seasonal predictions for the European energy industry. *Environmental Research Letters*, 12(2):024002, January 2017. ISSN 1748-9326. doi:10.1088/1748-9326/aa57ab.

de Groot, W. J., Wotton, B. M., and Flannigan, M. D. Wildland fire danger rating and early warning systems. In Shroder, J. F. and Paton, D., editors, *Wildfire Hazards, Risks and Disasters*, chapter 11, pages 207–228. Elsevier, Oxford, 2015. ISBN 978-0-12-410434-1. doi:10.1016/B978-0-12-410434-1.00011-7.

Dharssi, I., Vidale, P. L., Verhoef, A., Macpherson, B., Jones, C., and Best, M. New soil physical properties implemented in the unified model at PS18. Technical Report 528, Met Office, Exeter, UK, January 2009. URL https://digital.nmla.metoffice.gov.uk/IO_01baed78-35d1-426d-aad0-88357bb493b2.

Eastaugh, C. S., Arpaci, A., and Vacik, H. A cautionary note regarding comparisons of fire danger indices. *Nat. Hazards Earth Syst. Sci.*, 12(4):927–934, April 2012. doi:10.5194/nhess-12-927-2012.

EROS Archive. Global topographic 30 arc-second hydrologic digital elevation model 1 km, 2017. URL http://doi.og/10.5066/f77p8wn0.

Fasullo, J. T., Otto-Bliesner, B. L., and Stevenson, S. ENSO's changing influence on temperature, precipitation, and wildfire in a warming climate. *Geophys. Res. Lett.*, 45(17):9216–9225, 2018. doi:10.1029/2018GL079022.

Giglio, L., Randerson, J. T., and van der Werf, G. R. Analysis of daily, monthly, and annual burned area using the fourth-generation global fire emissions database (GFED4). *Journal of Geophysical Research: Biogeosciences*, 118(1):317–328, 2013. doi:10.1002/jgrg.20042.

Gilham, R. Met Office JULES fire module version 1.0 (JULES v4.1). Technical note attached to JULES Ticket #5, December 2014. URL https://code.metoffice.gov.uk/trac/jules/attachment/ticket/5/JULES_fire_docs_vn4.1.pdf.

Golding, N. and Betts, R. Fire risk in Amazonia due to climate change in the HadCM3 climate model: Potential interactions with deforestation. *Global Biogeochem. Cycles*, 22(4):GB4007, December 2008. doi:10.1029/2007gb003166.

Hamadeh, N., Karouni, A., Daya, B., and Chauvet, P. Using correlative data analysis to develop weather index that estimates the risk of forest fires in Lebanon & Mediterranean: Assessment versus prevalent meteorological indices. *Case Stud. Fire Safety*, 7:8–22, 2017. doi:10.1016/j.csfs.2016.12.001.

Hansen, J., Sato, M., Ruedy, R., Kharecha, P., Lacis, A., Miller, R. L., Nazarenko, L., Lo, K., Schmidt, G. A., Russell, G., Aleinov, I., Bauer, S., Baum, E., Cairns, B., Canuto, V., Chandler, M., Cheng, Y., Cohen, A., Del Genio, A., Faluvegi, G., Fleming, E., Friend, A., Hall, T., Jackman, C., Jonas, J., Kelley, M., Kiang, N. Y., Koch, D., Labow, G., Lerner, J., Menon, S., Novakov, T., Oinas, V., Perlwitz, J. P., Perlwitz, J., Rind, D., Romanou, A., Schmunk, R., Shindell, D., Stone, P., Sun, S., Streets, D., Tausnev, N., Thresher, D., Unger, N., Yao, M., and Zhang, S. Dangerous human-made interference with climate: A GISS modelE study. *Atmos. Chem. Phys.*, 7:2287–2312, 2007. doi:10.5194/acp-7-2287-2007.

Heinsch, F. A., Maosheng Zhao, Running, S. W., Kimball, J. S., Nemani, R. R., Davis, K. J., Bolstad, P. V., Cook, B. D., Desai, A. R., Ricciuto, D. M., Law, B. E., Oechel, W. C., Hyojung Kwon, Hongyan Luo, Wofsy, S. C., Dunn, A. L., Munger, J. W., Baldocchi, D. D., Liukang Xu, Hollinger, D. Y., Richardson, A. D., Stoy, P. C., Siqueira, M. B. S., Monson, R. K., Burns, S. P., and Flanagan, L. B. Evaluation of remote sensing based terrestrial productivity from MODIS using regional tower eddy flux network observations. *IEEE Transactions on Geoscience and Remote Sensing*, 44(7):1908–1925, July 2006. doi:10.1109/TGRS.2005.853936.

Hoffmann, W. A., Schroeder, W., and Jackson, R. B. Regional feedbacks among fire, climate, and tropical deforestation. *J. Geophys. Res.*, 108(D23):4721, December 2003. ISSN 0148-0227. doi:10.1029/2003jd003494.

Holgate, C. M., van Dijk, A. I. J. M., Cary, G. J., and Yebra, M. Using alternative soil moisture estimates in the McArthur forest fire danger index. *International Journal of Wildland Fire*, 26(9):806, 2017. doi:10.1071/wf16217. URL https://doi.org/10.1071/wf16217.

Holsten, A., Dominic, A. R., Costa, L., and Kropp, J. P. Evaluation of the performance of meteorological forest fire indices for German federal states. *For. Ecol. Manage.*, 287:123–131, 2013. doi:10.1016/j.foreco.2012.08.035.

Jones, C. D. and Cox, P. M. On the significance of atmospheric CO_2 growth rate anomalies in 2002–2003. *Geophys. Res. Lett.*, 32(14):L14816, July 2005. doi:10.1029/2005gl023027.

Jones, C. D., Collins, M., Cox, P. M., and Spall, S. A. The carbon cycle response to ENSO: A coupled climate–carbon cycle model study. *J. Climate*, 14(21):4113–4129, November 2001. doi:10.1175/1520-0442(2001)014<4113:TCCRTE>2.0.CO;2.

Keetch, J. and Byram, G. A drought index for forest fire control. *US Department of Agriculture Forest Service Research Paper*, page 35, 1968. URL https://www.srs.fs.usda.gov/pubs/rp/rp_se038.pdf.

Kim, J.-S., Kug, J.-S., Yoon, J.-H., and Jeong, S.-J. Increased atmospheric CO_2 growth rate during El Niño driven by reduced terrestrial productivity in the CMIP5 ESMs. *J. Climate*, 2016. doi:10.1175/jcli-d-14-00672.1.

Le Quéré, C., Andrew, R. M., Friedlingstein, P., Sitch, S., Hauck, J., Pongratz, J., Pickers, P. A., Korsbakken, J. I., Peters, G. P., Canadell, J. G., Arneth, A., Arora, V. K., Barbero, L., Bastos, A., Bopp, L., Chevallier, F., Chini, L. P., Ciais, P., Doney, S. C., Gkritzalis, T., Goll, D. S., Harris, I., Haverd, V., Hoffman, F. M., Hoppema, M., Houghton, R. A., Hurtt, G., Ilyina, T., Jain, A. K., Johannessen, T., Jones, C. D., Kato, E., Keeling, R. F., Goldewijk, K. K., Landschützer, P., Lefèvre, N., Lienert, S., Liu, Z., Lombardozzi, D., Metzl, N., Munro, D. R., Nabel, J. E. M. S., Nakaoka, S.-I., Neill, C., Olsen, A., Ono, T., Patra, P., Peregon, A.,

Peters, W., Peylin, P., Pfeil, B., Pierrot, D., Poulter, B., Rehder, G., Resplandy, L., Robertson, E., Rocher, M., Rödenbeck, C., Schuster, U., Schwinger, J., Séférian, R., Skjelvan, I., Steinhoff, T., Sutton, A., Tans, P. P., Tian, H., Tilbrook, B., Tubiello, F. N., van der Laan-Luijkx, I. T., van der Werf, G. R., Viovy, N., Walker, A. P., Wiltshire, A. J., Wright, R., Zaehle, S., and Zheng, B. Global carbon budget 2018. *Earth System Science Data*, 10(4):2141–2194, 2018. doi:10.5194/essd-10-2141-2018.

Lin, C.-C. Study on the predicting system of forest fire danger rating in taiwan. *Bull. Taiwan Forest Res. Inst.*, 10(3):325–330, 1995. URL https://www.tfri.gov.tw/main/science_in.aspx?mnuid=5470&modid=3&cid=152&cid2=873&nid=2960.

Luke, R. H. and McArthur, A. G. *Bush fires in Australia.* Australian Government Publishing Service, Canberra, 1978.

MacLachlan, C., Arribas, A., Peterson, K. A., Maidens, A., Fereday, D., Scaife, A. A., Gordon, M., Vellinga, M., Williams, A., Comer, R. E., Camp, J., Xavier, P., and Madec, G. Global Seasonal forecast system version 5 (GloSea5): a high-resolution seasonal forecast system. *Q. J. R. Meteor. Soc.*, 141(689):1072–1084, April 2015. doi:10.1002/qj.2396.

Mangeon, S., Voulgarakis, A., Gilham, R., Harper, A., Sitch, S., and Folberth, G. INFERNO: a fire and emissions scheme for the UK Met Office's Unified Model. *Geosci. Model Dev.*, 9(8):2685–2700, August 2016. doi:10.5194/gmd-9-2685-2016.

Mariani, M., Fletcher, M. S., Holz, A., and Nyman, P. ENSO controls interannual fire activity in southeast Australia. *Geophys. Res. Lett.*, 43:10891–10900, January 2016. doi:10.1002/2016gl070572.

McArthur, A. G. Weather and grassland fire behaviour. Forestry and Timber Bureau, Leaflet No. 100, Department of National Development, Canberra, 1966.

Noble, I. R., Gill, A. M., and Bary, G. A. V. Mcarthur's fire-danger meters expressed as equations. *Austral Ecology*, 5(2):201–203, June 1980. doi:10.1111/j.1442-9993.1980.tb01243.x.

Pachavo, G. and Murwira, A. Remote sensing net primary productivity (NPP) estimation with the aid of GIS modelled shortwave radiation (SWR) in a Southern African savanna. *Int. J. Appl. Earth Obs. Geoinform.*, 30:217–226, 2014. doi:10.1016/j.jag.2014.02.007.

Page, S., Siegert, F., Rieley, J., Boehm, H., Jaya, A., and Limin, S. The amount of carbon released from peat and forest fires in Indonesia during 1997. *Nature*, 420 (6911):61–65, 2002. doi:10.1038/nature01131.

Palin, E. J., Scaife, A. A., Wallace, E., Pope, E. C. D., Arribas, A., and Brookshaw, A. Skilful seasonal forecasts of winter disruption to the UK transport system. *J. Appl. Meteorol. Clim.*, 55(2):325–344, February 2016. doi:10.1175/jamc-d-15-0102.1.

Philander, S. G. *El Niño, La Niña, and the Southern Oscillation.* Number 46 in International Geophysics. Academic Press, 1990. ISBN 978-0-12-553235-8. URL https://www.sciencedirect.com/bookseries/international-geophysics/vol/46/suppl/C.

Randerson, J. T., Chen, Y., van der Werf, G. R., Rogers, B. M., and Morton, D. C. Global burned area and biomass burning emissions from small fires. *Journal of Geophysical Research: Biogeosciences*, 117(G4), 2012. doi:10.1029/2012JG002128. URL https://agupubs.onlinelibrary.wiley.com/doi/abs/10.1029/2012JG002128.

Randerson, J., Van der Werf, G., Giglio, L., Collatz, G., and Kasibhatla, P. Global fire emissions database, version 4.1 (GFEDv4), 2017. URL https://daac.ornl.gov/cgi-bin/dsviewer.pl?ds_id=1293.

Ren, H.-L., Scaife, A. A., Dunstone, N., Tian, B., Liu, Y., Ineson, S., Lee, J.-Y., Smith, D., Liu, C., Thompson, V., Vellinga, M., and MacLachlan, C. Seasonal predictability of winter ENSO types in operational dynamical model predictions. *Clim. Dynam.*, 52(7):3869–3890, April 2019. doi:10.1007/s00382-018-4366-1.

Rodenbeck, C., Zaehle, S., Keeling, R., and Heimann, M. History of El Niño impacts on the global carbon cycle 1957–2017: a quantification from atmospheric CO_2 data. *Philosophical Transactions of the Royal Society B-Biological Sciences*, 373(1760), 2018. doi:10.1098/rstb.2017.0303.

Roxburgh, S. H., Berry, S. L., Buckley, T. N., Barnes, B., and Roderick, M. L. What is NPP? inconsistent accounting of respiratory fluxes in the definition of net primary production. *Functional Ecology*, 19(3):378–382, 2005. doi:10.1111/j.1365-2435.2005.00983.x.

Scaife, A. A., Comer, R. E., Dunstone, N. J., Knight, J. R., Smith, D. M., MacLachlan, C., Martin, N., Peterson, K. A., Rowlands, D., Carroll, E. B., Belcher, S., and Slingo, J. Tropical rainfall, Rossby waves and regional winter climate predictions. *Q. J. R. Meteor. Soc.*, 143(702):1–11, January 2017. doi:10.1002/qj.2910.

Scaife, A. A., Ferranti, L., Alves, O., Athanasiadis, P., Baehr, J., Dequé, M., Dippe, T., Dunstone, N., Fereday, D., Gudgel, R. G., Greatbatch, R. J., Hermanson, L., Imada, Y., Jain, S., Kumar, A., MacLachlan, C., Merryfield, W., Müller, W. A., Ren, H.-L., Smith, D., Takaya, Y., Vecchi, G., and Yang, X. Tropical rainfall predictions from multiple seasonal forecast systems. *Int. J. Climatol.*, 39(2):974–988, February 2019. doi:10.1002/joc.5855.

Sirakoff, C. A correction to the equations describing the McArthur forest fire danger meter. *Australian Journal of Ecology*, 10(4):481–481, 1985. doi:10.1111/j.1442-9993.1985.tb00909.x.

Skvarenina, J., Mindas, J., Holecy, J., and Tucek, J. Analysis of the natural and meteorological conditions during two largest forest fire events in the Slovak Paradise National Park. In Xanthopoulos, G., editor, *Proceedings of the International Scientific Workshop on Forest Fires in the Wildland–Urban Interface and Rural Areas in Europe: an integral planning and management challenge*, pages 29–36, 15–16 May 2003, Athens, Greece, 2004. Mediterranean Agronomic Institute of Chania, Chania, Greece. URL http://www.fria.gr/WARM/warmProceedings.htm.

Slevin, D., Tett, S. F. B., Exbrayat, J.-F., Bloom, A. A. A., and Williams, M. Global evaluation of gross primary productivity in the JULES land surface model v3.4.1. *Geosci. Model Dev.*, 10(7):2651–2670, 2017. doi:10.5194/gmd-10-2651-2017.

Spessa, A. C., Field, R. D., Pappenberger, F., Langner, A., Englhart, S., Weber, U., Stockdale, T., Siegert, F., Kaiser, J. W., and Moore, J. Seasonal forecasting of fire over Kalimantan, Indonesia. *Natural Hazards and Earth System Sciences*, 15(3):429–442, 2015. doi:10.5194/nhess-15-429-2015.

Trenberth, K. E. The definition of El Niño. *Bull. Am. Meteorol. Soc.*, 78(12):2771–2778, 1997. doi:10.1175/1520-0477(1997)078<2771:TDOENO>2.0.CO;2.

Turco, M., Jerez, S., Doblas-Reyes, F. J., AghaKouchak, A., Llasat, M. C., and Provenzale, A. Skilful forecasting of global fire activity using seasonal climate predictions. *Nat. Commun.*, 9(1):2718, 2018. doi:10.1038/s41467-018-05250-0.

van der Werf, G. R., Randerson, J. T., Giglio, L., van Leeuwen, T. T., Chen, Y., Rogers, B. M., Mu, M., van Marle, M. J. E., Morton, D. C., Collatz, G. J., Yokelson, R. J., and Kasibhatla, P. S. Global fire emissions estimates during 1997–2016. *Earth System Science Data*, 9(2):697–720, 2017. doi:10.5194/essd-9-697-2017.

Walsh, S. F., Nyman, P., Sheridan, G. J., Baillie, C. C., Tolhurst, K. G., and Duff, T. J. Hillslope-scale prediction of terrain and forest canopy effects on temperature and near-surface soil moisture deficit. *International Journal of Wildland Fire*, 26 (3):191, 2017. doi:10.1071/wf16106. URL `https://doi.org/10.1071/wf16106`.

Walters, D., Boutle, I., Brooks, M., Melvin, T., Stratton, R., Vosper, S., Wells, H., Williams, K., Wood, N., Allen, T., Bushell, A., Copsey, D., Earnshaw, P., Edwards, J., Gross, M., Hardiman, S., Harris, C., Heming, J., Klingaman, N., Levine, R., Manners, J., Martin, G., Milton, S., Mittermaier, M., Morcrette, C., Riddick, T., Roberts, M., Sanchez, C., Selwood, P., Stirling, A., Smith, C., Suri, D., Tennant, W., Vidale, P. L., Wilkinson, J., Willett, M., Woolnough, S., and Xavier, P. The Met Office Unified Model Global Atmosphere 6.0/6.1 and JULES Global Land 6.0/6.1 configurations. *Geosci. Model Dev.*, 10(4):1487–1520, April 2017. doi:10.5194/gmd-10-1487-2017.

Weedon, G. P., Gomes, S., Viterbo, P., Shuttleworth, W. J., Blyth, E., Österle, H., Adam, J. C., Bellouin, N., Boucher, O., and Best, M. Creation of the WATCH forcing data and its use to assess global and regional reference crop evaporation over land during the Twentieth Century. *J. Hydrometeorol.*, 12(5):823–848, October 2011. doi:10.1175/2011jhm1369.1.

Weedon, G. P., Balsamo, G., Bellouin, N., Gomes, S., Best, M. J., and Viterbo, P. The WFDEI meteorological forcing data set: WATCH forcing data methodology applied to ERA-Interim reanalysis data. *Water Resour. Res.*, 50(9):7505–7514, September 2014. doi:10.1002/2014wr015638.

Williams, K. D., Harris, C. M., Bodas-Salcedo, A., Camp, J., Comer, R. E., Copsey, D., Fereday, D., Graham, T., Hill, R., Hinton, T., Hyder, P., Ineson, S., Masato, G., Milton, S. F., Roberts, M. J., Rowell, D. P., Sanchez, C., Shelly, A., Sinha, B., Walters, D. N., West, A., Woollings, T., and Xavier, P. K. The Met Office Global Coupled model 2.0 (GC2) configuration. *Geosci. Model Dev.*, 8(5):1509–1524, May 2015. doi:10.5194/gmd-8-1509-2015.

Williams, K. E. and Falloon, P. D. Sources of interannual yield variability in JULES-crop and implications for forcing with seasonal weather forecasts. *Geosci. Model Dev.*, 8(12):3987–3997, 2015. doi:10.5194/gmd-8-3987-2015.

Zeng, N., Mariotti, A., and Wetzel, P. Terrestrial mechanisms of inter-annual CO_2 variability. *Global Biogeochemical Cycles*, 19:GB1016, 2005. doi:10.1029/2004GB002273.

Zhao, M., Running, S. W., and Nemani, R. R. Sensitivity of moderate resolution imaging spectroradiometer (MODIS) terrestrial primary production to the accuracy of meteorological reanalyses. *Journal of Geophysical Research: Biogeosciences*, 111 (G1):G01002, 2006. doi:10.1029/2004JG000004.